Validation and Strategies to Improve the Hydro-Estimator and NEXRAD over Puerto Rico

NAZARIO D. RAMIREZ-BELTRAN
Department of Industrial Engineering
University of Puerto Rico
P.O. Box 9030, Mayagüez, PR 00681
U.S.A
nazario@ece.uprm.edu

ROBERT J. KULIGOWSKI
NOAA/NESDIS Center for Satellite Applications and Research (STAR)
Camp Springs, MD 20746
U.S.A.
Bob.Kuligowski@noaa.gov

ERIC W. HARMSEN
Department of Agricultural and Biosystems Engineering
University of Puerto Rico
P.O. Box 9030, Mayagüez, PR 00681
U.S.A.
eharmsen@uprm.edu

JOAN M. CASTRO
Department of Computer and Electrical Engineering
University of Puerto Rico
P.O. Box 9030, Mayagüez, PR 00681
U.S.A
joanmanuelcastro@yahoo.com

SANDRA CRUZ-POL
Department of Computer and Electrical Engineering
University of Puerto Rico
P.O. Box 9040, Mayagüez, PR 00681
U.S.A
SandraCruzPol@ieee.org

MELVIN J. CARDONA-SOTO
Department of Computer and Electrical Engineering
University of Puerto Rico
P.O. Box 9030, Mayagüez, PR 00681
U.S.A
cardonam@gmail.com

Abstract - Validation of the Hydro-Estimator (HE) and the Next Generation Radar (NEXRAD) during heavy storms over Puerto Rico (PR) is reported. The HE is a high resolution rainfall retrieval algorithm based on satellite and numerical whether prediction model data. The accuracy of the HE and the NEXRAD rainfall estimates can be measured by decomposing the rainfall process in sequences of discrete (rain / no rain) and continuous (rainfall rate) random variables. Validation results are based on five heavy storms that seriously impacted human life and the economy of PR during the period 2003 to 2005. The average discrete validation results indicate acceptable hit rate values for both the HE and NEXRAD (0.76 vs. 0.87) and reasonable discrete bias ratios (1.04 vs. 0.73) but a very low of probability of detection of rain for both the HE and NEXRAD (0.36 vs. 0.52). The HE shows an average overestimation whereas the NEXRAD exhibits underestimation in the continuous validation results (continuous bias ratio of 1.14 vs 0.70 for NEXRAD), which contributes to moderate overall errors for the HE and NEXRAD in terms of root mean squared error (2.14 mm vs. 1.66 mm) and mean absolute error (0.96 mm vs. 0.77 mm).

The HE algorithm was designed to operate over US continental areas and satisfactory results have been reported. However, over tropical regions it was determined that warm clouds can generate substantial rainfall amounts that are not detected by the HE algorithm. Infrared band differencing techniques are using to explore the possibility of improving the detection of warm-cloud rain events over PR. We are also classifying clouds based on Geostationary Operational Environmental Satellite (GOES) Imager data in a manner that will lead to improved relationships between infrared brightness temperatures and rainfall rates.

Key-words - validation, NEXRAD, Hydro-Estimator, retrieval algorithm, rain rate, GOES, brightness temperature.

1. Introduction

Estimation of rainfall amounts is critical for protecting human lives and infrastructure, particularly in the case of heavy rainfall that triggers flash floods or landslides. In Puerto Rico (PR) during 2003 to 2005, five severe storms seriously impacted human lives and the economy. PR has extremely diverse terrain, and during the rainy season severe rainstorms can develop due to complex orographic attributes. Easterly winds come from the eastern Atlantic almost all year and play an important role in bringing humidity into the island and stimulating orographic rainfall over the mountains of PR.   Cold fronts dominate the weather pattern during wintertime. Tropical waves occur during the rainy season and frequently generate large amounts of rainfall in the Caribbean basin. These tropical waves are typically the precursor of tropical storms and hurricanes from June to November.

For these types of events, estimates of rainfall from instruments on geostationary platforms such as the Geostationary Operational Environmental Satellite (GOES) are preferred over microwave-based estimates of rainfall from Low-Earth-Orbiting (LEO) platforms because of the rapid refresh every 15 minutes over the Continental United States (CONUS) and nearby regions and very short data latency times of GOES data relative to low-Earth orbit data. Numerous algorithms have been developed to estimate precipitation from GOES-based satellite data.   The current generation of algorithms produced at the National Oceanic and Atmospheric Administration (NOAA) National Environmental Satellite,

Data and Information Service (NESDIS) are the Hydro-Estimator (HE, [1]), GOES Multi-Spectral Rainfall Algorithm (GMSRA, [2]), and the Self-Calibrating Multivariate Precipitation Retrieval (SCaMPR, [3]). The HE relies on GOES data from the infrared (IR) window channel (10.7 μm) with a fixed relationship to rainfall rates; similarly, Palmeira et al. [4] presented a self-consistent algorithm for rainfall estimation based on GOES data plus lightning data in Brazil. The GMSRA uses additional data from three other GOES channels and updates its calibration in real time based on matches with radar rain rates. SCaMPR calibrates GOES IR parameters against passive microwave rain rates, which is an approach similar to Kidd et al. [5] and the Precipitation Estimation from Remotely Sensed Information using Artificial Neural Network (PERSIANN, [6]) algorithm. PERSIANN uses the combined geostationary infrared and the Tropical Rainfall Measuring Mission (TRMM) microwave information to estimate rainfall rate in an hourly basis at spatial resolution of 0.25°. Another algorithm called the CPC Morphing Algorithm (CMORPH, [7]) also combines IR data and microwave rain rates, but uses the IR data as the basis for interpolating the microwave rain rates in time between low-Earth orbit satellite overpasses.

The HE, which will be the focus of this paper, also uses information from numerical whether prediction models to estimate rain rate [1]. Rainfall rates are adjusted upward or downward for moist or dry environments as indicated by National Centers for Environmental Prediction (NCEP) North American Model (NAM) or Global Forecast System (GFS) total column precipitable

water and mean-layer relative humidity for the lowest third of the model vertical domain. Another adjustment enhances rainfall rates in regions where the convective equilibrium level temperature is relatively high; i.e., regions where very cold cloud tops are not thermodynamically possible but where strong updrafts and heavy rainfall can still occur. Finally, low-level winds and digital topography are combined to produce enhancements of rainfall rates in upslope regions and reductions in downslope regions, using a technique described in Vicente et al. [8].

The HE has been the operational satellite rainfall algorithm of the National Environmental Satellite, Data, and Information Service (NESDIS) since 2002 and produces rainfall estimates at the full spatial and temporal resolution of GOES over the CONUS and surrounding regions, including PR; real-time estimates are also produced on an experimental basis for the rest of the globe. However, validation of the Hydro-Estimator has generally focused on the CONUS (e.g., [1] and [9]) and has not been performed over Puerto Rico, and given the differences in topography and climate of Puerto Rico relative to the CONUS, previous validation efforts may not necessarily be relevant to users in PR. Furthermore, validation of the HE over PR may illuminate opportunities to enhance the algorithm for application over PR.

Validation of the rainfall retrieval algorithm consists of comparing the rainfall estimates with corresponding observations (rain gauges in this study). The accuracy of rainfall estimates can be measured by decomposing the rainfall process as sequences of discrete and continuous random variables; i.e., the presence or absence of rainfall events (discrete variable) and the amount of rainfall (continuous variable). The occurrence of rainfall events in a given area and at a particular time follows a Bernoulli process and consequently the estimation accuracy of rainfall events can be conducted by analyzing a contingency table. The typical scores that measure the accuracy of categorical forecasts are: hit rate (H), probability of detection (POD), false-alarm rate (FAR), and discrete bias (DB). The continuous validation strategy consists of comparing the amount of rainfall that occurred at specific area in a particular time and the continuous measurements of accuracy are: mean absolute error (MAE), root mean squared error (RMSE), and continuous bias (CB).

The second section of this paper describes the data collection process and source of information. The third section describes the conventional statistical techniques to perform validation. The fourth section presents validation results during heavy storms over PR, and includes a comparison for rain gauges versus HE and rain gauges versus NEXRAD. The fifth section presents some strategies for algorithm improvements. The sixth section presents some conclusions.

2. Data collection

Puerto Rico has a rain gauge network that collects rainfall measurements every 5, 10, 15, 30 or 45 minutes and includes 125 rain gauges with data available since January 2000. Since the majority of gauges collect rainfall every 15 minutes a computer program was designed to derive HE and NEXRAD 15 minutes resolution. The rain gauge data are used to perform validation of the HE and the NEXRAD. The data set used for validation includes five heavy storms that have been impacted PR: Three can be characterized as a cold front and two as tropical storms.

NEXRAD data over Puerto Rico come from a WSR-88D unit located in Cayey (18.12°N, 66.08°W, 886.63 m elevation). The radar frequency is 2.7 GHz and the maximum horizontal range is 462.5 km, and the radar scans the entire island every 6 minutes. The NOAA National Severe Storms Laboratory (NSSL) conducted a significant effort to make possible an affordable nationwide operational capture, distribution, and archiving of Level II NEXRAD data [10]. Unfortunately, for Puerto Rico the Level II data are available only until 2003 with a significant amount of missing data in that last year [11]. The NWS did resume archiving level II data for PR during the summer of 2007. On the other hand, Level III data for PR are available continuously since 2000 [12], so the Level III data were selected to perform validation since the most recent and catastrophic floods over PR occurred after 2002. The scanning angle for reflectivity data was selected as 0.5 degrees for this research in order to avoid beam overshoot over western PR. Fig. 1 shows the location of the radar and the spatial distribution of the rain gauges.
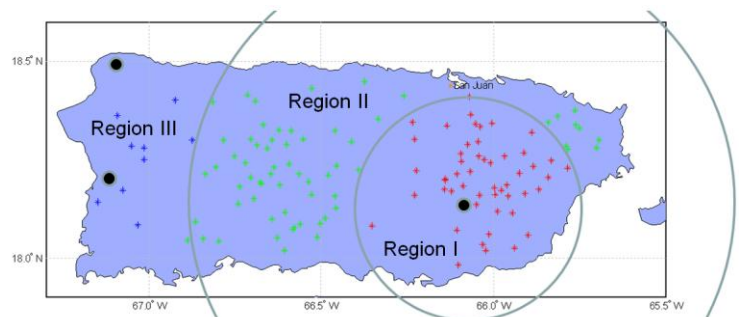

FIG. 1. Location of rain gauges (stars) and NEXRAD (black dot on Region I) in PR. Black dots in Region III are small and high resolution radar that will be used to derive the bias correction factor for NEXRAD. The radii of the circles are 35 km and 90 km.

As mentioned in the Introduction, the HE uses satellite IR window (10.7 μm) data and numerical whether prediction data to estimate rainfall over the CONUS and PR every 15 minutes at 4 km spatial resolution, and they are available for the entire period of interest. In order to ensure consistency among these data sets during the

comparison, both the NEXRAD and HE rain rates were aggregated in time over the corresponding 15-minute accumulation period of the gauges.

3. Validation techniques

Validation of the rainfall retrieval algorithm consists of comparing the rainfall estimates with observations over the same time and space. The accuracy of rainfall estimates can be measured by decomposing the rainfall process into sequences of discrete and continuous random variables, i.e., the presence or absence of rainfall events and the amounts of rainfall. The occurrence of rainfall events in a given area and at a particular time follows a Bernoulli process and consequently the estimation accuracy of rainfall events can be conducted by analyzing contingency tables, bivariate probability distribution of rainfall events [13]. Table 1 shows the classical two-way contingency table.

It is assumed that the values provided by the rain gauges are the "ground truth" while the HE and the NEXRAD provide estimated rainfall values. The variable a in the contingency table is the number of times that the rain gauge identifies a rainfall event and the estimator also correctly identifies a rainfall event at the same time and space. The variable d represents the number of times the rain gauge does not observe a rainfall event and the estimator correctly determines that there is no rainfall event. The variable b indicates the number of times the rain gauge does not observe a rainfall event but the estimator incorrectly indicates that there is a rainfall event. The variable c shows the number of times that the rain gauge detects a rainfall event but the estimator incorrectly does not detect the rainfall event.

TABLE 1. Sample contingency table.

		Observed rainfall (Rain gauge)	
		Yes	No
Estimated rainfall	Yes	a	b
(HE or NEXRAD)	No	c	d

The typical scores that measure the accuracy of categorical estimation are:

$$H = \frac{a+d}{n_o}, \quad \text{where} \quad n_o = a+b+c+d \quad (1)$$

$$POD = \frac{a}{a+c} \quad (2)$$

$$FAR = \frac{b}{a+b} \quad (3)$$

$$DB = \frac{a+b}{a+c} \quad (4)$$

where H is the hit rate, POD is the probability of detection, FAR is the false-alarm rate, and DB is the discrete bias. Hit rate is the fraction of the n_o estimating occasions when the categorical estimation correctly determines the occurrence of rainfall event or nonevent. Probability of detection is the likelihood that the event would be estimated, given that it occurred. The false-alarm rate is the proportion of estimated rainfall events that fail to materialize. Bias is the ratio of the number of estimated rainfall events to the number of observed events [13].

The continuous validation strategy consists of comparing the amount of rainfall that occurred with the estimated amount of rainfall at specific area in a particular time and the continuous accuracy scores used here are:

$$e_{ij} = y_{ij} - \hat{y}_{ij} \quad i = 1,\ldots,n \quad \text{and} \quad j = 1,\ldots,m \quad (5)$$

$$MAE = \frac{1}{n\,m} \sum_{i=1}^{n} \sum_{j=1}^{m} |e_{ij}| \quad (6)$$

$$RMSE = \sqrt{\frac{1}{n\,m} \sum_{i=1}^{n} \sum_{j-1}^{m} e_i^2} \quad (7)$$

$$CB = \frac{\sum_{i=1}^{n} \sum_{j=1}^{m} \hat{y}_{ij}}{\sum_{i=1}^{n} \sum_{j=1}^{m} y_{ij}} \quad (8)$$

where y and $\hat{y}$ are the observed and estimated amount of rainfall. The i and j subscripts represent time and space, respectively. The constant n is the total number of time intervals for a given storm, and m is the number of rain gauges that are collecting rain during a storm. The error e is the deviation between the observed and estimated amount of rainfall at a particular time and space and is computed only when at least one of y or $\hat{y}$ is greater than zero. MAE is the mean absolute error, $RMSE$ the root mean squared error, and CB is the continuous bias.

4. Validation results

4.1 Discrete validation
A contingency table was computed for each rain gauge during a given storm and the scores of those tables were summarized to create contingency tables for each storm for the HE and NEXRAD which are shown in Tables 2a) and 2b) while the associated scores are given in Tables 3a) and 3b). The HE significantly underestimates the number of

raining pixels in the three April-May events (DB of 0.49 to 0.52) but strongly overestimates the November-December events (DB of 1.54 and 2.15). The physical reasons behind this apparent strong seasonal variation in DB are not known at this time. Meanwhile, the NEXRAD had a consistent dry bias (0.62-0.68) for the last four events but virtually no bias (1.02) for the first; again, it is not clear at this time what led to such a significant difference. The hit rates of the HE range from 0.62 to 0.91 with an average of 0.76 and NEXRAD has a range from 0.82 to 0.95 with average of 0.87. Although, both HE and NEXRAD exhibit relatively high hit rate, the HE has a lower percentage of correct rain / no rain estimates than does the NEXRAD. The probability of detection of the HE ranges from 0.14 to 0.57 with an average value of 0.36, whereas, the NEXRAD shows a range from 0.4 to 0.74 with an average of 0.52. Thus, the HE correctly detected a smaller percentage of the observed rainfall events (36%) than did NEXRAD (52%) for these events. The false alarm rate for the HE varies between 0.39 to 0.73 with an average value of 0.61, meanwhile the NEXRAD varies from 0.25 to 0.35 with an average of 0.29. Thus, the false alarm rate was actually higher for the HE (61%) than for NEXRAD (29%). Thus, the discrete validation shows that the NEXRAD outperforms the HE in terms of correct rain / no rain estimates.

TABLE 2. Contingency tables for (a) the Hydro-Estimator and (b) NEXRAD.

a)

17 April 2003		Rain Gauge	
		Yes	No
Hydro-Estimator	Yes	1105	699
	No	2603	6708

19-21 May, 2003		Rain Gauge	
		Yes	No
Hydro-Estimator	Yes	331	875
	No	2000	30022

11-18 November, 2003		Rain Gauge	
		Yes	No
Hydro-Estimator	Yes	10430	18719
	No	8465	47913

5 December 2003		Rain Gauge	
		Yes	No
Hydro-Estimator	Yes	4882	13224
	No	3538	23167

20 April 2005		Rain Gauge	
		Yes	No
Hydro-Estimator	Yes	310	395
	No	1039	8522

b)

17 April 2003		Rain Gauge	
		Yes	No
NEXRAD	Yes	2713	951
	No	1023	6311

19-21 May, 2003		Rain Gauge	
		Yes	No
NEXRAD	Yes	1177	1149
	No	399	30386

11-18 November 2003		Rain Gauge	
		Yes	No
NEXRAD	Yes	8922	9967
	No	3620	62901

5 December 2003		Rain Gauge	
		Yes	No
NEXRAD	Yes	3392	5026
	No	1814	34462

20 April 2005		Rain Gauge	
		Yes	No
NEXRAD	Yes	655	670
	No	240	8583

TABLE 3. Discrete validation scores for the Hydro-Estimator and NEXRAD.

a)

	17 Apr. 2003	19-21 May 2003	11-18 Nov. 2003	5 Dec. 2003	20 Apr. 2005	Avg.
DB	0.49	0.52	1.54	2.15	0.52	1.04
HR	0.70	0.91	0.68	0.62	0.86	0.76
POD	0.30	0.14	0.55	0.57	0.23	0.36
FAR	0.39	0.72	0.64	0.73	0.56	0.61

b)

	17 Apr. 2003	19-21 May 2003	11-18 Nov. 2003	5 Dec. 2003	20 Apr. 2005	Avg.
DB	1.02	0.68	0.66	0.62	0.67	0.73
HR	0.82	0.95	0.84	0.85	0.91	0.87
POD	0.74	0.51	0.47	0.40	0.49	0.52
FAR	0.27	0.25	0.29	0.35	0.27	0.29

4.2 Continuous validation

The accumulated rainfall across the island was computed to compare the observed and the estimated rainfall:

$$Y_i = \sum_{j=1}^{m} y_{ij} \quad i = 1, 2, \cdots, n \quad (9)$$

where Y_i is the total rainfall recorded by all 125 rain gauges across the island or the closest HE or radar pixels at the ith time.

Tables 4a) and 4b) show the continuous validation scores for HE and NEXRAD, respectively. The continuous bias of the HE is even more variable than the

DB, with values ranging from 0.16-0.26 for the April-May storms and 1.68-2.42 for the November-December events. The lower CB relative to the DB for the April-May storms suggests that the HE is underestimating the conditional rainfall rates in addition to the spatial extent of the rainfall, while the opposite is happening for the November-December events. The NEXRAD has nearly no continuous bias for two storms and a strong dry bias for three (0.41-0.68), albeit with no apparent seasonal pattern like the HE. As a result, both the mean absolute error and root mean squared error of the HE are also higher than that of NEXRAD.

Table 4. Continuous validation scores for the Hydro-Estimator and NEXRAD.

a)	17 Apr. 2003	19-21 May 2003	11-18 Nov. 2003	5 Dec. 2003	20 Apr. 2005	Avg.
CB	0.26	0.23	1.68	2.42	0.16	0.95
MAE (mm)	1.33	0.74	1.10	0.86	0.79	0.96
RMSE (mm)	2.73	2.10	2.24	1.93	1.71	2.14

b)	17 Apr. 2003	19-21 May, 2003	11-18 Nov. 2003	5 Dec. 2003	20 Apr. 2005	Avg.
CB	1.02	0.68	0.41	0.42	1.01	0.71
MAE (mm)	1.02	0.66	0.85	0.53	0.80	0.77
RMSE (mm)	1.91	1.79	1.78	1.15	1.68	1.66

5. Algorithm improvements

5.1 Rainfall detection

As stated previously, the HE uses GOES brightness temperatures (Tb) from channel 4 (10.7 µm) to discriminate raining from non-raining events [1]. During the validation exercise we noted that there are some warm-top convective events that are not detected by the HE. The HE generally produces little or no rainfall for brightness temperatures exceeding 235K; however, there are numerous events in PR where the HE largely failed to detect significant rainfall. For instance, Fig. 2 shows the observed accumulated rainfall for all gauges located in PR (red line) and the accumulated rainfall by the corresponding HE pixels (blue line) on November 14, 2006. The horizontal axes shows the time every 15 minutes and the vertical axis exhibits the accumulated rainfall in mm. Fig. 3 shows the distribution of brightness temperatures over the GOES pixels corresponding to gauge locations during this storm and there are few pixels below 235 K; a comparison with Fig. 2 indicates that the poor detection by the HE was at least in part because it was not calibrated to produce rainfall from relatively warm clouds. In order to improve the detection skill of the HE, we plan to examine the differences in brightness temperature between 10.7 µm and the water vapor band (6.5 µm in GOES-12). Positive values of the WV-infrared window temperature difference have been shown to

correspond with convective cloud tops that are above the tropopause (i.e. overshooting tops), ([14 and [15]). Convective clouds with positive differences indicate the possibility of warm-top convection. We will also explore the use of the reflected portion of the 3.9-µm GOES band 2 during the daytime to indicate the presence large cloud-top particles that suggest rain in warm-top clouds [2].
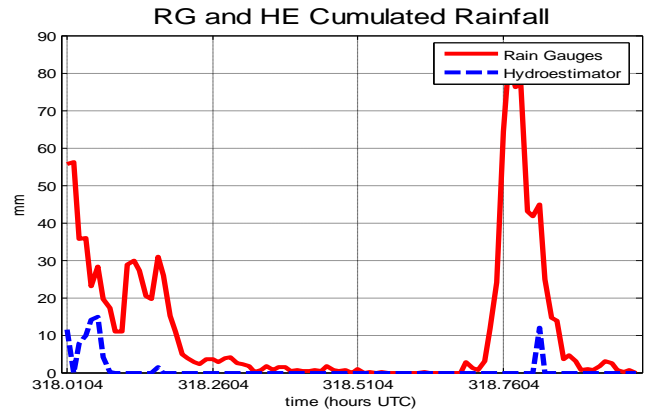

FIG. 2. Comparison between observed and estimated accumulated rainfall (Nov. 14, 2006).
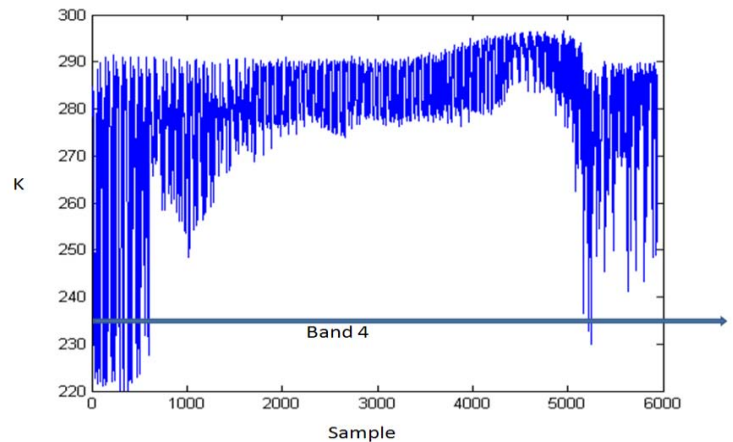

FIG. 3. GOES-12 brightness temperature from channel 4 (Nov. 14, 2006).

5.2 Improving rain rate estimates

The rainfall retrieval procedure of the HE is also mainly based on the relationship between the brightness temperature (10.7 µm) and observed rain rate. Estimation of the amount of rainfall may be improved by classifying the brightness temperature patterns (BTP) with the corresponding rain formation processes. The following channels will be used to classify the BTP with the corresponding rain process. Channel 1 (0.65 µm) will be used to classify the events according to the cloud optical thickness. The reflected portion of channel 2 (3.9 µm) during the daytime will be used as an indirect measurement of the cloud drop size distribution, thermodynamic phase, and particle shape [16]. Channel 4

(10.7 μm) will be used to classify the rainfall events according to temperature. The infrared band differencing will also be used to develop the classification algorithm. The difference between the 10.7-µm brightness temperature and 3.9-µm will be useful to determine whether a cloud top is composed of liquid water or ice. As stated previously, the IR-WV difference (6.5–10.7 µm) is usually negative; however, convective clouds with positive differences have likely already begun to precipitate, especially in tropical atmospheres that support warm top convection. The 13.3–10.7 µm differencing technique is used to characterize and delineate cumulus clouds. This research will focus on convective clouds, and consequently, the factors to be consider for the classification of BTP and rain types are: area, depth, duration, and updraft velocity.

A variable selection algorithm will be used to identify the variables that best explain the rainfall variability, and the selected variables will be used to develop the training patterns for a self-organized artificial neural network [17]. A self-organized artificial neural network will be used to identify a set of homogenous groups that reveal similarities within the member of a class, but different among the classes. The Kohonen learning rule will be used to determining the optimal weights of the artificial neural network ([18], [19], and [20]). A successful application was reported [21] to identify the spatial variability of soil to select the appropriate model to estimate soil moisture.

6   Summary and conclusions

The HE is a high resolution satellite rainfall retrieval algorithm run operationally by NOAA/NESDIS that provides estimates of rainfall every 15 minutes at 4-km resolution over the CONUS and nearby areas including PR. (Global estimates are also produced in real time on an experimental basis.) The rain rates are primarily derived from GOES 10.7-µm brightness temperatures and then adjusted using parameters derived from a numerical weather prediction model. The HE estimates should be especially useful over regions of complex topography such as western PR because of the difficulties associated with radar in those regions such as beam block. However, for the very small sample of heavy rainfall events examined in this paper, NEXRAD clearly outperforms the HE, perhaps in part because of most of the rainfall events were located in the central and eastern parts of the island where the radar data will be most reliable. Specifically, the HE underestimates both the number of rainfall events and the amounts of rainfall, whereas NEXRAD is nearly unbiased in these respects. The HE algorithm does exhibit a satisfactory hit rate, but a very low probability of detection and a large false alarm rate that is surprisingly higher than that of NEXRAD despite the dry bias of the HE. A research effort is undergone to improve the performance of the HE for PR; specifically, the algorithm proposed by Ramirez-Beltran et al. [17] will be implemented to improve the HE rainfall detection and the equation that relates brightness temperatures with rain rates.

7   Acknowledgements.

References

[1] Scofield, R.A., and R.J. Kuligowski, 2003: Status and outlook of operational satellite precipitation algorithms for extreme-precipitation events. Wea. *Forecasting,* **18**, 1037-1051.

[2] Ba, M. B., and A. Gruber, 2000: GOES Multispectral Rainfall Algorithm (GMSRA). *J. Appl. Meteor.*, **40**, 1500-1514.

[3] Kuligowski, R.J., 2002: A Self-Calibrating real-time GOES rainfall algorithm for short-term rainfall estimates. *J. Hydrometeor.*, **3**, 112-130.

[4] Palmeira, F. L. B., C. A. Morales, G. B. França, and L. Landau, 2004: Rainfall estimation using satellite data for Paraíba do Sul Basin (Brazil). *The XXth ISPRS International Society for Photogrammetry and Remote Sensing Congress*, Istanbul, Turkey - Commission 7.

[5] Kidd, C., Kniveton, D.R., Todd, M.C., Bellerby, T.J., 2003: Satellite Rainfall Estimation Using Combined Passive Microwave and Infrared Algorithms. *J. Hydrometeor.*, **4**, 1088-1104.

[6] Sorooshian, S., K.-L. Hsu, X. Gao, H. V. Gupta, B. Imam, and D. Braithwaite, 2000: An evaluation of PERSIANN system satellite-based estimates of tropical rainfall. *Bull. Amer. Meteor. Soc.*, **81**, 2035-2046.

[7] Joyce, R.J., J. E. Janowiak, P.A. Arkin, and P. Xie, 2004: CMORPH: A method that produces global precipitation estimates from passive microwave and infrared data at high spatial and temporal resolution. *J. Hydrometeor.*, **5**, 487-503.

[8] Vicente, G. A., J. C. Davenport, and R. A. Scofield, 2001: The role of orographic and parallax corrections on real time high resolution satellite rainfall rate distribution. *Int. J. Remote Sens.*, **23**, 221-230.

[9] Ebert, E. E., J. E. Janowiak, and C. Kidd, 2007: Comparison of near-real-time precipitation estimates from satellite observations and

numerical models. *Bull. Amer. Meteor. Soc.*, **88**, 47-64.

[10] Kelleher, K.E., K. K. Droegemeier, J. J. Levit, C. Sinclair, D. E. Jahn, S. D. Hill, L. Mueller, G. Qualley, T. D. Crum, S. D. Smith, S. A. Del Greco, S. Lakshmivarahan, L. Miller, M. Ramamurthy, B. Domenic, and D. W. Fulker, 2007: A real-time delivery system for NEXRAD Level II data via the internet. *Bull. Amer. Meteor. Soc.*, **88**, 1045-1057.

[11] NCDC, 2005a: National Climatic Data Center: Data Documentation for DSI – 6500 – *NEXRAD Level II*. NCDC, Asheville, NC.

[12] NCDC, 2005b: National Climatic Data Center: Data Documentation for DSI – 7000 – *NEXRAD Level III*. NCDC, Asheville, NC.

[13] Wilks, D.S., 1995: *Statistical Methods in the Atmospheric Sciences: An Introduction.* Academic Press, San Diego, 467 pp.

[14] Ackerman, S. A., 1996: Global satellite observations of negative brightness temperature differences between 11 and 6.7 mm. *J. Atmos. Sci.*, **53**, 2803-2812.

[15] Schmetz, J., H. P. Roesli and W. P. Menzel, 1997: Third International Winds Workshop (Meeting summary). *Bull. Amer. Meteor. Soc.*, **78**, 893 – 896.

[16] Arking, A., and J. D. Childs, 1985: Retrieval of cloud cover parameters from multispectral satellite images. J. Climate Appl. Meteor., 24,

[17] Ramirez-Beltran, N.D., W.K.M. Lau, A. Winter, J.M. Castro, and N.R. Escalante, 2007: Empirical probability models to predict precipitation levels over Puerto Rico stations. *Mon. Wea. Rev*. 135, 877-890.

[18] Hagan, T.H., Demuth, H.B., and Beal, M., 1996: Neural Network Design, PWS Publishing Co., Boston.

[19] Ramirez-Beltran, N.D. and Montes, J.A. 2002: Neural networks to model dynamic systems with time delays. *IIE Transactions*, 34, 313-327.

[20] Ramirez-Beltran, N.D., and A. Veneros 2004: Upper air information and neural networks to estimate hurricane intensity. Preprints, *26th Conference on Hurricanes and Tropical Meteorology*. Miami FL.

[21] Ramírez Beltran, N.D, J. M. Castro., E. Harmsen, and R. Vasquez. 2008: Stochastic transfer function models and neural networks to estimate soil moisture. *J. of the Amer. Water Resources Assoc.* in press.